More Frequent, Longer, and Hotter Heat Waves for Australia in the Twenty-First Century

TIM COWAN AND ARIAAN PURICH

CSIRO Marine and Atmospheric Research, Aspendale, Victoria, Australia

SARAH PERKINS

Australian Research Council Centre of Excellence for Climate Systems Science, University of New South Wales, Sydney, New South Wales, Australia

ALEXANDRE PEZZA, GHYSLAINE BOSCHAT, AND KATHERINE SADLER

School of Earth Sciences, University of Melbourne, Melbourne, Victoria, Australia

(Manuscript received 30 January 2014, in final form 16 April 2014)

ABSTRACT

Extremes such as summer heat waves and winter warm spells have a significant impact on the climate of Australia, with many regions experiencing an increase in the frequency and duration of these events since the mid-twentieth century. With the availability of Coupled Model Intercomparison Project phase 5 (CMIP5) climate models, projected changes in heat waves and warm spells are investigated across Australia for two future emission scenarios. For the historical period encompassing the late twentieth century (1950–2005) an ensemble mean of 15 models is able to broadly capture the observed spatial distribution in the frequency and duration of summer heat waves, despite overestimating these metrics along coastal regions. The models achieve a better comparison to observations in their simulation of the temperature anomaly of the hottest heat waves. By the end of the twenty-first century, the model ensemble mean projects the largest increase in summer heat wave frequency and duration to occur across northern tropical regions, while projecting an increase of ~3°C in the maximum temperature of the hottest southern Australian heat waves. Model consensus suggests that future winter warm spells will increase in frequency and duration at a greater rate than summer heat waves, and that the hottest events will become increasingly hotter for both seasons by century's end. Even when referenced to a warming mean state, increases in the temperature of the hottest events are projected for southern Australia. Results also suggest that following a strong mitigation pathway in the future is more effective in reducing the frequency and duration of heat waves and warm spells in the southern regions compared to the northern tropical regions.

1. Introduction

Heat waves are a common occurrence across many heavily populated regions of the world, including southern and central Europe (e.g., Fischer and Schar 2010; Kyselý 2010; Carril et al. 2008; Della-Marta et al. 2007; Trigo et al. 2005), North America (e.g., Bumbaco et al. 2013; Wu et al. 2012b; Mastrandrea et al. 2011), China (Wu et al. 2012a; Ding et al. 2007), Russia (Trenberth and Fasullo 2012; Barriopedro et al. 2011), central and southern Africa (Hao et al. 2013; Lyon 2009), and southern Australia (Bureau of Meteorology 2013; Lewis and Karoly 2013; Nairn and Fawcett 2013; Tryhorn and Risbey 2006). These types of events are often characterized by consecutive days above a threshold maximum temperature; in some definitions, they also incorporate a distinct lack of nighttime temperature relief with consecutive nights above a minimum temperature threshold (Pezza et al. 2012; Nairn and Fawcett 2013).

For Australia, heat waves occur in all seasons and are often referred to as warm spells in austral winter. Based on the maximum temperature definition of heat waves from Perkins and Alexander (2013), across the central interior and tropical regions where summer temperatures are high (often exceeding 35°C), but daily variability is

Corresponding author address: Tim Cowan, CSIRO Marine and Atmospheric Research, PMB1, Aspendale VIC 3195, Australia.
E-mail: tim.cowan@csiro.au

DOI: 10.1175/JCLI-D-14-00092.1

low, there are about two heat wave events per extended summer; however, such events tend to only be ~2°–4°C warmer than the climatological maximum temperature. For southern Australia, a region of great agricultural importance and where more than a third of Australia's population live, one to two summer heat waves occur on average annually; however, such events can be up to 15°C warmer than the climatological maximum (Perkins and Alexander 2013). This is because the southern latitudes experience a high frequency of synoptic prefrontal weather systems (Tryhorn and Risbey 2006), causing more severe heat waves to develop due to the greater variability of summer temperatures (Nairn and Fawcett 2013). Heat waves in the Australian midlatitude regions are often triggered by atmospheric processes such as breaking Rossby waves and persistent anticyclones (Pezza et al. 2012; Perkins and Alexander 2013; Marshall et al. 2014; Parker et al. 2013), which allow advection of warm air over the affected region. The anticyclones are often accompanied by a low pressure trough or tropical depression over the northwest of Australia (Hudson et al. 2011; Pezza et al. 2012), which may directly reinforce the downstream anticyclone (Parker et al. 2013).

Recent observations suggest that the frequency, duration, and intensity of heat wave events are increasing over land regions across the globe (e.g., Coumou and Rahmstorf 2012, and references therein), including many regions of Australia (Pezza et al. 2012; Perkins et al. 2012; Perkins and Alexander 2013). Despite various limitations in simulating regional changes (Hao et al. 2013), climate models project these trends to continue with increasing emissions of greenhouse gases (Coumou and Robinson 2013; Meehl and Tebaldi 2004). There is also considerable evidence to suggest that anthropogenic forcings have contributed to recent extreme heat wave events across the Northern Hemisphere (Hansen et al. 2012) and to record warm summer temperatures across Australia (Lewis and Karoly 2013). According to Coupled Model Intercomparison Project phase 5 (CMIP5) climate models, the likelihood of a human contribution to the extreme Australian summer of 2012/13 has been assessed to be ~2.5–5 times greater than that without greenhouse warming (Lewis and Karoly 2013). CMIP5 models also project a severalfold increase in global monthly heat extremes by the mid-twenty-first century (Coumou and Robinson 2013). This follows on from large increases (decreases) in the warm/dry (cold/wet) extremes across many tropical and subtropical regions throughout the late twentieth century, which are well captured by the CMIP5 models (Hao et al. 2013). However, a comprehensive and detailed assessment of how future warming will impact heat waves across Australia using CMIP5 climate model simulations has yet to be undertaken.

We therefore investigate the projected changes in heat waves across Australia in the twenty-first century, comparable to the analysis of Perkins and Alexander (2013), which examined observed trends. The importance of understanding how trends in heat wave metrics will change in a warming world is underscored by the impact these extreme events have on human health and mortality. Numerous studies have detailed the increased risk of heat-related deaths due to extreme heat events in populated regions of Europe (Le Tertre et al. 2006), North America (Zanobetti and Schwartz 2008), and Australia (e.g., Loughnan et al. 2010; Tong et al. 2010). Based on little or no acclimatization, this risk will likely increase severalfold by the late twenty-first century (Gosling et al. 2009). Therefore, communities require greater certainty in understanding the risk of increased heat waves in the future and a better understanding as to whether mitigation will reduce the likelihood of extreme heat conditions (as in Coumou and Robinson 2013).

For this study, we define Australian heat waves as summer-only events, as this is when they have the greatest impact on human health (e.g., Pezza et al. 2012) because of their intensity, as well as influencing other extreme events such as bushfires (Karoly 2009). However, we also examine winter warm spells to investigate the seasonality of the projected changes. CMIP5 data are used to examine how heat wave and warm spell frequency, duration, and hottest event anomalies across Australia will change under two emission scenarios over the twenty-first century.

2. Data and methods

Daily maximum and minimum temperatures (T_{max} and T_{min}, respectively) are utilized for the historical (1950–2005) and future (2006–2100) periods. Observations over the historical period are taken from the Bureau of Meteorology high-resolution gridded (0.05° × 0.05°) temperature dataset (Jones et al. 2009). This dataset has been used previously to investigate several heat wave metric trends over the late twentieth century (Perkins and Alexander 2013). Fifteen CMIP5 models listed in Table 1 that have daily T_{max} and T_{min} from the historical experiment and two representative concentration pathway (RCP) experiments [RCP4.5 (medium-low emission scenario) and RCP8.5 (high emission scenario)] are analyzed (Taylor et al. 2012).

The CMIP5 models are bilinearly interpolated to a 2° × 2° grid, as the median resolution of the models used is ~1.9°. For consistency, the observations are also interpolated to the same grid. As with Perkins and Alexander (2013) the choice of grid resolution (0.5° × 0.5°, 1° × 1°, or 2° × 2°) for observations is found not to affect results (not shown).

TABLE 1. CMIP5 models and simulations used in this study.

Model	Modeling group
ACCESS1.0 (Australian Community Climate and Earth-System Simulator, version 1.0)	Commonwealth Scientific and Industrial Research Organisation (CSIRO) and Bureau of Meteorology (BoM), Australia
ACCESS1.3 (Australian Community Climate and Earth-System Simulator, version 1.3)	CSIRO and BoM, Australia
CanESM2 (Second Generation Canadian Earth System Model)	Canadian Centre for Climate Modelling and Analysis (CCCma), Canada
CNRM-CM5 (Centre National de Recherches Météorologiques Coupled Global Climate Model, version 5)	Centre National de Recherches Météorologiques (CNRM) and Centre Européen de Recherche et de Formation Avancée en Calcul Scientifique (CERFACS), France
CSIRO Mk3.6.0 (Commonwealth Scientific and Industrial Research Organisation Mark, version 3.6.0)	CSIRO and Queensland Climate Change Centre of Excellence (QCCE), Australia
GFDL CM3 (Geophysical Fluid Dynamics Laboratory Climate Model, version 3)	National Oceanic and Atmospheric Administration (NOAA) Geophysical Fluid Dynamics Laboratory (GFDL), United States
GFDL-ESM2G [Geophysical Fluid Dynamics Laboratory Earth System Model with Generalized Ocean Layer Dynamics (GOLD) component]	NOAA GFDL, United States
GFDL-ESM2M [Geophysical Fluid Dynamics Laboratory Earth System Model with Modular Ocean Model 4 (MOM4) component]	NOAA GFDL, United States
HadGEM2-CC (Hadley Centre Global Environment Model, version 2–Carbon Cycle)	Met Office Hadley Centre (MOHC), United Kingdom
MIROC-ESM (Model for Interdisciplinary Research on Climate, Earth System Model)	Japan Agency for Marine-Earth Science and Technology (JAMSTEC), Atmosphere and Ocean Research Institute (AORI), and National Institute for Environmental Studies (NIES), Japan
MIROC-ESM-CHEM (Model for Interdisciplinary Research on Climate, Earth System Model, Chemistry Coupled)	JAMSTEC, AORI, and NIES, Japan
MIROC5 (Model for Interdisciplinary Research on Climate, version 5)	AORI, NIES, and JAMSTEC, Japan
MPI-ESM-LR (Max Planck Institute Earth System Model, low resolution)	Max Planck Institute (MPI), Germany
MRI-CGCM3 (Meteorological Research Institute Coupled Atmosphere–Ocean General Circulation Model, version 3)	Meteorological Research Institute (MRI), Japan
NorESM1-M [Norwegian Earth System Model, version 1 (intermediate resolution)]	Norwegian Climate Centre (NCC), Norway

For this study, a heat wave is defined as a period during which T_{max} exceeds a threshold temperature for three or more consecutive days, and T_{min} exceeds a threshold temperature on the second and third days (Pezza et al. 2012). This definition takes into account that heat waves have the most severe effects on human health when there is a lack of relief between hot days, and is similar to previous studies (e.g., Della-Marta et al. 2007; Carril et al. 2008; Lau and Nath 2012). Two different T_{max} and T_{min} thresholds based on the 1950–2005 climatology are tested:

1) monthly 90th percentile T_{max} and T_{min}, where all days in a heat wave are referenced to temperatures from the month of first heat wave day (Pezza et al. 2012); and
2) daily 90th percentile T_{max} and T_{min}, calculated for each day using a centered 15-day window (i.e., 7 days before and after a calendar day) (Perkins and Alexander 2013).

The results from both threshold definitions are found not to be substantially different with respect to the modeled heat wave metric biases (not shown). Based on their similarity, the remainder of the paper uses the monthly climatology threshold definition.

For each grid point, heat wave dates occurring during austral summer (December–February) are determined and analyzed using three main heat wave metrics (as in Perkins and Alexander 2013):

1) heat wave frequency (HWF), the number of heat wave days per summer;
2) heat wave duration (HWD), the length of the longest summer heat wave event;[1] and

[1] By definition, HWD must be ≥3 days and is defined as a missing value in summers without a heat wave. Likewise, HWA is defined as a missing value for summers without a heat wave. However, for such summers HWF is defined as zero, and thus averaging over time can result in HWF < 3 days.

3) heat wave amplitude (HWA), the anomaly of the hottest day of the hottest summer heat wave (based on T_{max}).

Two additional heat wave metrics are also described in Perkins and Alexander (2013):

1) heat wave number, the number of heat wave events per summer; and
2) heat wave magnitude, the average daily intensity of summer heat waves.

However for brevity, as the climatologies and changes for heat wave number and magnitude are similar to HWF and HWA, respectively, results for these metrics are not presented.

The same procedure is also undertaken for austral winter (June–August) warm spells, as well as for austral autumn (March–May) and spring (September–November) events. For simplicity, in this manuscript the same acronyms for metrics corresponding to summer heat waves are used for winter warm spells (i.e., HWF is used to describe both heat wave frequency during summer and warm spell frequency during winter).

Historical summer heat wave and winter warm spell statistics at each grid point across Australia are used to construct observed and multimodel mean (MMM) composites of each metric over 1950–2005. Future heat wave and warm spell statistics at each grid point across Australia are also used to construct MMM composites over 2081–2100, for the two RCP emission scenarios, and the change relative to the historical period is presented. Statistical significance in these RCP minus historical composite maps is assessed using a two-tailed Mann–Whitney U test (Mann and Whitney 1947). This nonparametric test determines whether the 2081–2100 composite is distinguishable from the 1950–2005 composite at the 95% confidence level.

We also assess how simulated heat wave conditions for the populated southern Australian cities of Sydney, Melbourne, and Perth evolve over 1950–2100. This is achieved using daily T_{max} and T_{min} interpolated to the three cities airport locations for Sydney (33.9°S, 151.2°E), Melbourne (37.6°S, 144.8°E), and Perth (31.9°S, 116.0°E). Averaged time series from the four grid points surrounding the airport locations are also assessed and found to be comparable to those from interpolated airport locations (not shown). Time series of HWF and HWD for these cities are presented, and based on the ability of CMIP5 models to simulate continental-wide historical heat wave statistics, we have confidence in simulations of heat wave changes at the finer spatial scale. Such time series allow the evolution of the heat wave changes to be viewed, and the differences between RCP scenarios for particular locations to be examined in depth. In each of the time series presented, the historical and future changes are based on a multimodel mean with the error based on the 95% confidence interval.

3. Results

a. Observed summer heat wave climatology

Over 1950–2005, the observations show that much of central and southeast Australia (incorporating the agriculturally important Murray–Darling basin) experiences >2.5 heat wave days per summer (Fig. 1a), equivalent to ~1 event per season (not shown). Along the coastal fringes of Australia the HWF drops to <1.5 days per summer. This spatial pattern compares well to the regional variations in HWF found using slightly less constrained definitions of heat waves in Perkins and Alexander (2013). Using only the 90th percentile T_{max} to describe heat waves, Perkins and Alexander (2013) calculated an HWF of 8–10 days per extended summer for central and southeast Australia, whereas heat waves defined using only the 90th percentile T_{min} show an HWF of 4–6 days per extended summer. The difference compared to the climatologies shown here may be a combination of different definitions and the fact that Perkins and Alexander (2013) analyze heat waves over an extended 5-month summer (November–March), where greater heat wave numbers would be expected.

The spatial pattern of observed HWD does not directly follow that of HWF: the longest heat waves across the midlatitude regions of Australia are shorter than those in central and tropical northern regions (Fig. 1b). This supports previous work suggesting that prefrontal activity in southern Australia results in shorter heat waves, compared to the continental interior (Tryhorn and Risbey 2006). South of 30°S, the HWD is ~3–4 days, which, for Melbourne, is slightly less than that calculated from station data (Pezza et al. 2012), whereas in the central and northern tropics the HWD is 5–6 days. Along the western and eastern coastal subtropics, HWD is also ~3 days, perhaps reflecting coastal air–sea processes, such as sea breezes that prevent minimum temperatures from exceeding their "warm" threshold (Pezza et al. 2012).

In direct contrast, HWA is greatest over the southern latitudes (south of 25°S), and along the southern coastal fringes it is often >10°C warmer than the climatological T_{max} (Fig. 1c). HWA decreases equatorward, to ~3°C in the tropical north. This reflects the diverse nature of Australia's climate, which results in very little variability in heat extremes in the northern tropical summer (Nairn and Fawcett 2013), as well as a small diurnal cycle (Perkins and Alexander 2013), while across the southern

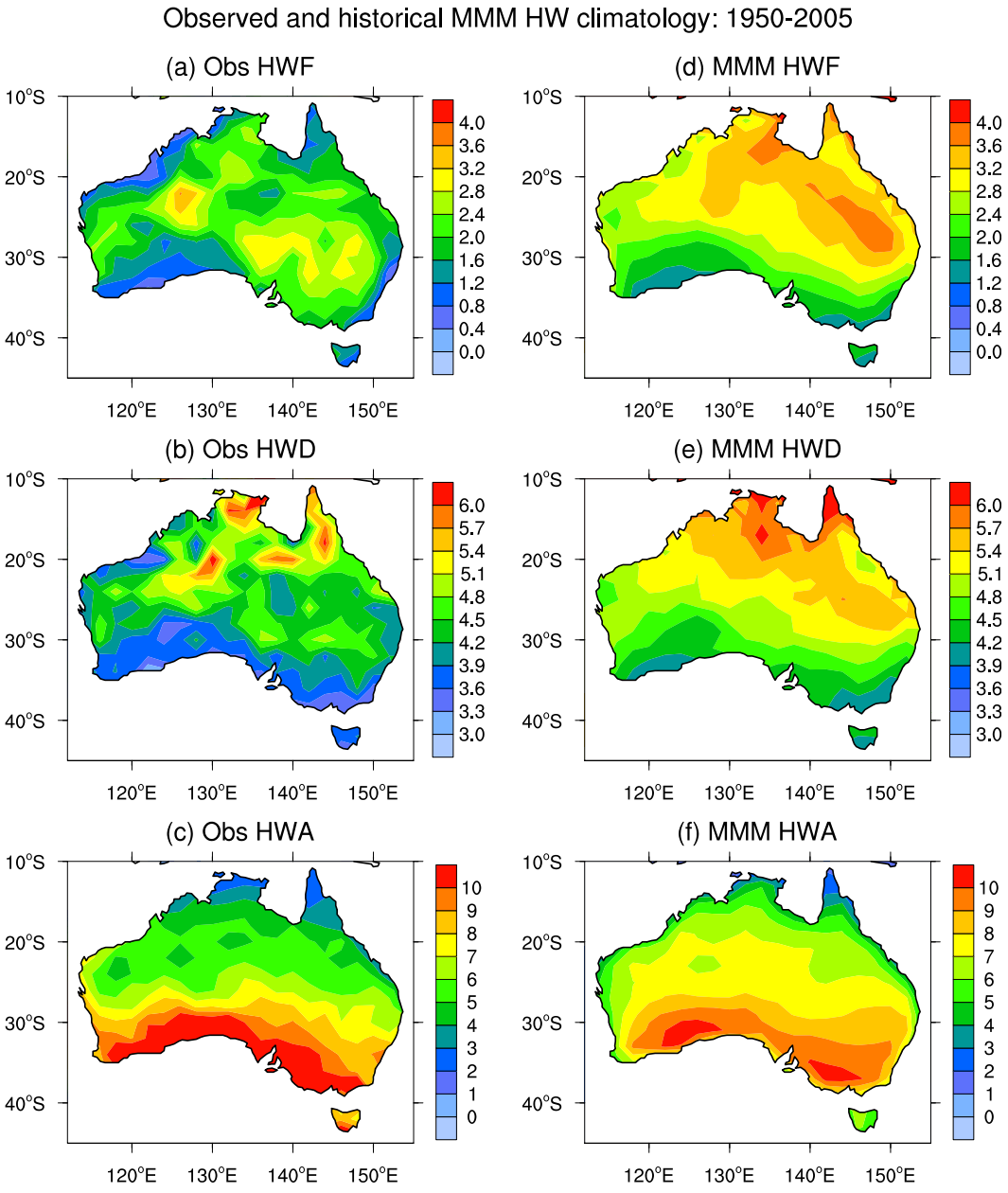

FIG. 1. Summer heat wave metric climatologies over 1950–2005 for (left) observations and (right) CMIP5 MMM: (a),(d) heat wave frequency (HWF; days per summer), (b),(e) heat wave duration (HWD; days), and (c),(f) heat wave amplitude (HWA; °C). Heat waves are referenced to monthly 90th percentile climatologies, based on the definition described in Pezza et al. (2012).

latitudes the variability in T_{max} is high due to the existence of frontal activity including anticyclonic blocking systems (Tryhorn and Risbey 2006). The overlap between high values of HWF and HWA across southeast Australia explains why this region experiences the most frequent and hottest heat waves across the continent, increasing its susceptibility to other extreme events such as major bushfires (Ellis et al. 2004).

b. *CMIP5 historical summer heat wave climatology*

We next assess how well the CMIP5 models simulate summer HWF, HWD, and HWA for Australia over the historical period. In general, the MMM is able to simulate the spatial climatological meridional gradient in HWF (Fig. 1d), displaying a greater (reduced) likelihood of heat waves in the central (southern coastal) region. The MMM simulates an HWF of <2 days per

summer for the southern Australian coastline, which is a slight underestimate (overestimate) for the southeast (southwest) region. The models also simulate the HWF maximum to be >3.5 days per summer over central-eastern Australia, 1–2 days per summer greater than observed. A positive HWF bias is also simulated along the northeastern tropical coast of Queensland, while the models fail to capture the HWF minimum to the east of the Great Dividing Range, which may be indicative of a failure to simulate the strong orographic-induced thermal gradients. The importance of orographic resolution has been shown for northern Europe, where modeled atmospheric blocking biases are reduced when model orography is more realistic (Berckmans et al. 2013), although correcting mean model biases can also improve blocking (Scaife et al. 2010). More broadly, the model representation of the continental-scale HWF pattern is overly zonal, with a general failure to capture observed orographic gradients and coastal variations. This may also be a result of varying orography among the models, as well as the regridding and multimodel averaging processes, which act as a spatial filter.

The broad bias across central eastern and coastal southern Australia is also seen in the HWD (Fig. 1e), with the models overestimating HWD by as much as 1 day. It should be noted, however, that for southeast Australia the gridded observations likely include biases compared to station-based data, as seen for Melbourne (Pezza et al. 2012). The MMM again shows a strong climatological meridional gradient, with HWD across southern Australia and Tasmania reaching 4.5 days, while for the northern tropics the HWD is >6 days. Again, the MMM fails to capture specific regional variations, including a strengthening gradient extending inland from eastern Australia and the northwest coast. However, individual models such as ACCESS1.3 and MIROC-ESM-CHEM (the model names are expanded in Table 1) are able to capture this spatial variability, suggesting that the multimodel averaging process possibly filters out localized features where zonal and meridional gradients are large (e.g., near coastal fringes and across mountainous terrain).

The MMM performs best at representing HWA, highlighted in Fig. 1f, with southern Australia exhibiting the hottest heat waves close to 10°C above the climatological T_{max}, although the extent of HWAs >10°C is less than seen in the observations (Fig. 1c). The HWA biases across northern tropical Australia tend to be small, although a slight positive bias exists across central Australia (~2°C), and a slight negative bias is present across coastal southwest Australia and the southern-central coast (i.e., South Australia). In general, the MMM is able to simulate the large thermal meridional gradient across the country, but tends to be too warm compared to observations in the central interior.

In summary, despite the relative coarseness of climate model grids, model simulations are able to capture the main broad spatial features of these events well, including the strong meridional gradients in HWF, HWD, and HWA; however, they show the greatest discrepancies where strong coastal and orographic gradients exist.

c. *Observed winter warm spell climatology*

Because of differences in the prevailing weather systems, the patterns for winter warm spell metrics across Australia are understandably different to summer heat waves. Austral winter is the cool, wet season for the southern midlatitudes, which experience an increased number of frontal systems as the subtropical high pressure ridge shifts equatorward (Timbal and Drosdowsky 2013; Kent et al. 2013) and remote modes of variability such as the Indian Ocean dipole and the southern annular mode have greater influence on weather systems (Risbey et al. 2009; Cai et al. 2011b). Along the Great Dividing Range (east coast) and southern regions, the winter HWF is <2 days per winter, reflecting the role of frontal weather systems passing through this region causing large temperature variations (Nicholls et al. 2010). Across tropical northern Australia, austral winter heralds the dry, warm season, with the interior of this region experiencing a HWF of 3–4 days per winter (equivalent to ~1 event) (Fig. 2a).

The pattern of the winter HWD exhibits quite a large degree of spatial variability (Fig. 2b). In regions such as southwest Australia and Tasmania, the longest warm spells are at the threshold of 3 days (events <3 days are not considered warm spells), while for the far tropical north the longest warm spells can last close to 6 days. However, many localized variations also exist. In regions where there are sparse observations, such as the northwest of Australia, a degree of caution should be noted as these regions are known for their poor data quality (Ummenhofer et al. 2011); however, results from a 21-member ensemble from the Community Earth System Model suggest that increasing HWF trends in this data-sparse region are possible (Perkins and Fischer 2013).

Winter HWA displays a maximum over central Australia (Fig. 2c), >6°C warmer than the climatological T_{max}. Compared to summer HWA, the equatorward shift in maximum HWA (cf. Figs. 2c and 1c) represents the seasonal movement in the high pressure belt, which sits at ~28°S in winter. This shift allows frontal systems to pass across coastal southwest and southeast Australia, reducing the winter HWA in these regions. The overlap

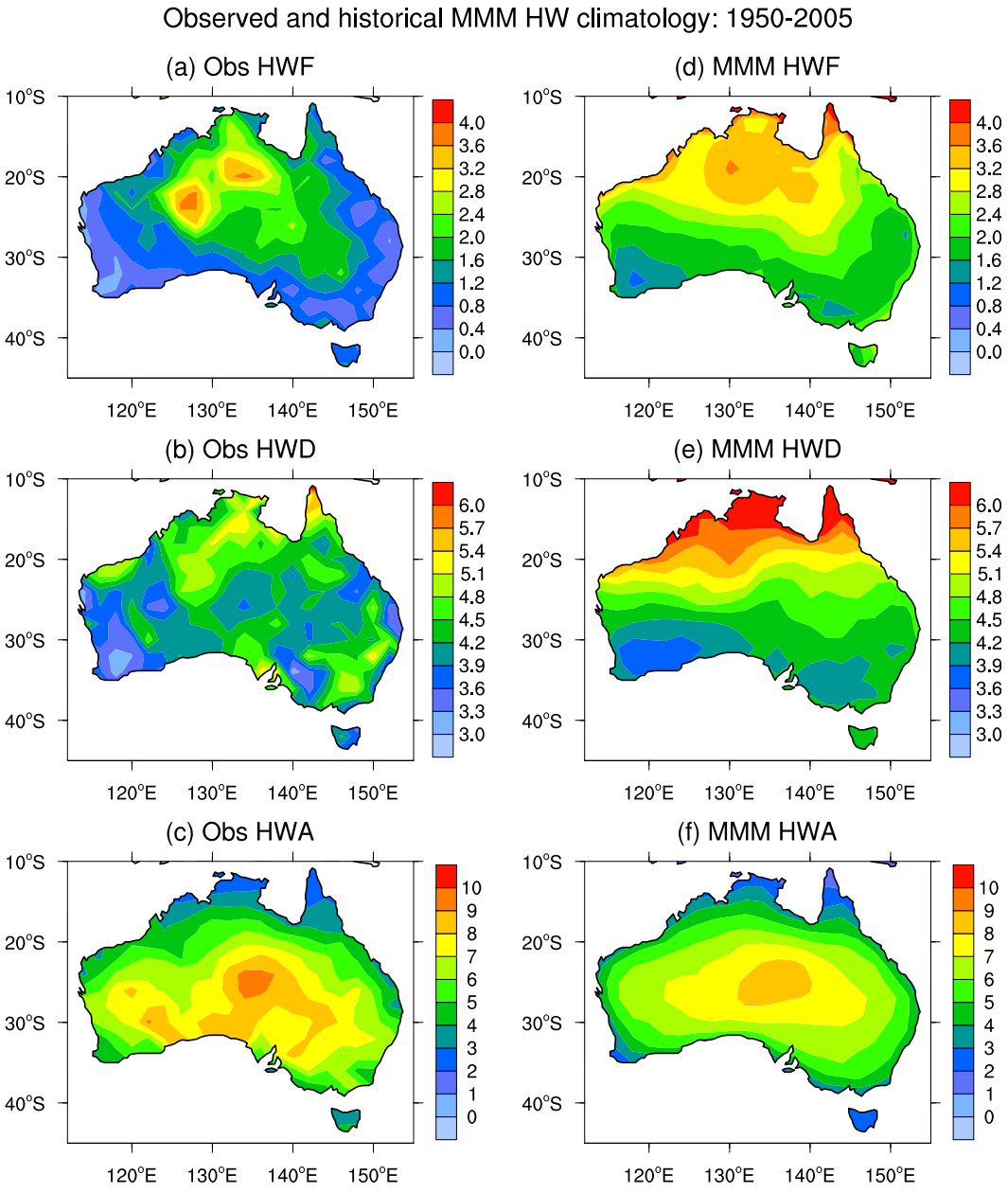

FIG. 2. As in Fig. 1, but for winter warm spells.

of high winter HWF, HWD, and HWA suggests that central Australia experiences the most intense and hottest warm spells during this season, as opposed to the continental southeast during summer.

d. CMIP5 historical winter warm spell climatology

In terms of winter HWF, the MMM captures the observed spatial shift in the maximum frequency relative to the summer HWF maximum. This frequency maximum for winter warm spells is located in northern Australia; the MMM performs well at capturing this (Fig. 2d). The MMM also captures the winter HWF minimums in the south and east, including along the east coast mountains (i.e., Great Dividing Range), but the frequency is overestimated with respect to the observations by ~1 day per winter. Localized regions, however, show the largest model biases, including the Cape York Peninsula in the tropical northeast, and the northwest coast (Pilbara region), with biases of >3 days per winter. These biases may relate to model uncertainty in how they represent local climatic features, but also could reflect uncertainties in the reliability of the

observations (Ummenhofer et al. 2011) and/or lack of data coverage (Jones et al. 2009).

For winter HWD, the largest biases of ~1 day are simulated across tropical northern Australia (Fig. 2e). The MMM spatial pattern exhibits a strong meridional gradient from the southern midlatitudes to the tropics, with winter HWD minimums captured across the southwest and southeast regions. The observations suggest strong zonal gradients exist for winter HWD, particularly along the mountainous east coast. While the MMM struggles to capture these regional variations, individual models such as GFDL-CM3 (not shown) perform well at simulating many of these observed regional characteristics.

As for summer, the MMM performs best at capturing the spatial climatology of the anomaly of the hottest winter warm spells (HWA) as shown in Fig. 2f. The MMM maximum occurs in central Australia, as seen in the observations, and represents an association with the seasonal equatorward shift in the high pressure belt associated with the contraction of the southern edge of Hadley cell (Nguyen et al. 2013). The MMM slightly underestimates the maximum winter HWA at 9°C (observed is 10°C). Furthermore, the MMM also underestimates the winter HWA in populated coastal regions of southwest and southeast Australia (including Tasmania), simulating an HWA of 3°C, whereas 5°–6°C is observed (Fig. 2c). In general, the models broadly capture the main winter features across Australia, including a greater frequency and duration of events across northern Australia compared to the south, as well at the hottest events in central Australia, coinciding with a shift in the subtropical pressure ridge. However, the models fail to capture some of the distinct regional gradients in warm spell metric patterns, particularly for HWD.

Confidence in these results allows us to evaluate how these heat wave and warm spell metrics may change throughout the twenty-first century, both from an overall continental perspective and at specific populated city locations. The changes in heat waves and warm spells as projected by the CMIP5 models with respect to two RCP scenarios are investigated in the next sections.

e. Future changes in summer heat waves

We next assess the continental-scale changes in heat wave metrics for the period 2081–2100, differenced from those of the historical period (1950–2005) for both the RCP4.5 and 8.5 scenarios. Figure 3 shows the patterns of change for summer heat waves for the end of the twenty-first century for HWF, HWD, and HWA. For RCP4.5, the HWF increases vary from 5–10 days per summer across southern regions to up to >25 days per summer in the tropical north (Fig. 3a). Given that the historical HWF for southern Australia is 1–2 days per summer (Fig. 1a), this implies a fivefold increase over the century, while for northern Australia the increase is closer to tenfold (although it should be noted that there is a positive MMM HWF bias in the historical period across the northern tropics of 1–3 days per summer). The patterns of change are also highly zonal in nature, with the meridional gradient of change being quite weak in the southern latitudes, and stronger in the northern tropics and along the northeastern Queensland coast. For RCP8.5, the meridional gradient across the subtropics and interior regions becomes much sharper (Fig. 3d); southern Australia HWF increases are between 10 and 20 days per summer, while increases over the 20°–30°S latitude band are in excess of 40 days per summer. Interestingly, changes in HWF over Tasmania do not follow the same pattern, where a 30-fold increase in HWF by 2100 relative to the historical period is projected. The results from both RCP4.5 and 8.5 suggest that HWF will increase at a greater magnitude further equatorward. As expected, this change is more extreme in RCP8.5 than for RCP4.5, implying that greenhouse warming strongly amplifies the frequency of heat wave events.

For HWD, the increase in RCP4.5 is >8 days in the tropical north and northeast, but only ~2 days south of 30°S (Fig. 3b). The pattern of change is predominantly zonal across the central interior. A strong gradient is projected for the tropical northeast, weakening away from the coastline. The pattern in the northern tropics implies that the length of future HWD will be more than 4 times the historical value, from 6 to ~25 days by the end of the century. For southern regions, the slight increase in the longest heat waves by 2 days by 2100 follows on from weak observed trends in HWD over 1950–2008 (Perkins and Alexander 2013). This suggests that the duration and frequency of southern Australian heat waves are less susceptible to anthropogenic warming than those in the tropical north, possibly due to the transient nature of the midlatitude anticyclones and cold fronts that pass through these regions (Tryhorn and Risbey 2006; Pezza et al. 2012). The latitude of these systems is strongly associated with the position of the subtropical high pressure belt and the southern edge of the Hadley cell.

The late-twenty-first century increase in HWD simulated in RCP8.5 represents an amplification of the RCP4.5 pattern, with increases >20 days in the tropical north and 2–4 days in southern regions (Fig. 3e). It should be noted that the large changes in the tropics are a result of relatively low variability in summer temperatures compared to the midlatitude regions. With very little variability in tropical heat (i.e., the distribution is narrow), even a modest warming of ~1°–2°C by 2100

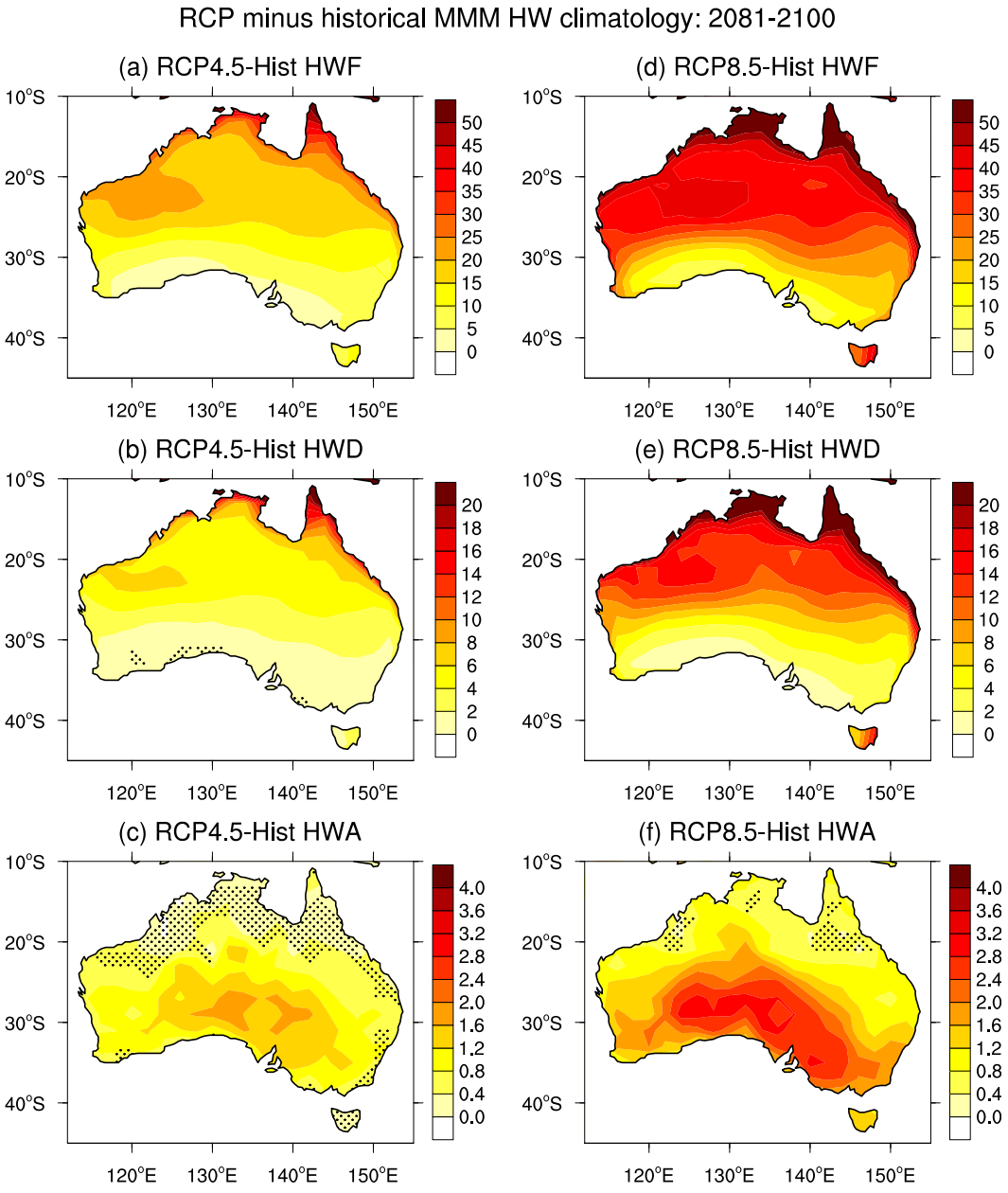

FIG. 3. Summer heat wave metric increases over 2081–2100, compared to the 1950–2005 climatology, for (left) RCP4.5 and (right) RCP8.5: (a),(d) HWF, (b),(e) HWD, and (c),(f) HWA. Stippling indicates where the 2081–2100 and 1950–2005 climatologies are *not* significantly different at the 95% confidence level (i.e., most regions are significant) based on a Mann–Whitney *U* test.

(Alexander et al. 2013) results in a larger increase in HWF and HWD compared to the southern regions. As such, future changes in HWF and HWD over tropical regions should be interpreted with caution (Perkins 2011), as noted for observed trends (Nairn and Fawcett 2013). As with the RCP8.5 HWF changes, the meridional gradient of change for HWD is much stronger than for RCP4.5, suggesting that an amplification of greenhouse warming is most influential on the spatial variations of heat waves. Again, trends over Tasmania oppose this pattern of change; however, it should be noted that the coarse resolution of the models places greater uncertainty over regions such as this island state, whose climate is influenced by its coastal and mountainous environment. As such climate downscaling is generally used to overcome these biases (Grose et al. 2010).

The patterns of change for HWA are opposite to those for HWF and HWD, showing large increases across central southern Australia of 3°C (>1.6°C) for the RCP8.5 (4.5) scenario (Figs. 3c,f). These changes reflect a broad amplification of the climatological pattern as observed and simulated in the historical period (Figs. 1c,f). Northern tropical Australia shows a weak and sometimes insignificant change (0.4°–0.8°C), possibly due to a limit in the temperature increases in humid, tropical areas where wet-bulb temperatures sometimes match actual temperatures (Sherwood and Huber 2010). The changes in the tropics also emphasize that due to the narrow distribution in summer temperatures, future mean-state warming has very little influence on HWA, yet HWF and HWD increase dramatically.

From this analysis it can be concluded that southern Australia will experience a moderate increase in the frequency and duration of discrete summer heat wave events in the future, but the heat waves will be significantly hotter than in the historical period. For the northern tropics and interior, heat waves will be significantly more frequent and longer, but only slightly warmer than those of the historical period. However, the lack of temperature variability in the tropics means one should not overinterpret these regional projections (e.g., Perkins 2011).

f. Summer time series of heat wave metrics

Given that the majority of Australia's population reside along the eastern seaboard and southern coasts, we next examine the evolution of heat wave metrics for selected city locations. The purpose of this is to understand the evolution of the projected change in these three metrics by the end of the twenty-first century with respect to the historical period (1950–2005) at single locations.

We compare HWF, HWD, and HWA for Sydney (eastern-southeast Australia), Melbourne (southern-southeast Australia), and Perth (southwest Australia). Sydney is situated in a temperate climate zone (warm, humid summers and mild winters, with high annual rainfall), but can be influenced by the tropical Pacific variability (Risbey et al. 2009). Melbourne experiences a maritime climate (warm summers and cool-to-cold winters with rainfall year-round), and Perth experiences a Mediterranean climate (hot, dry summers and cool, wet winters).

The simulated evolutions of the heat wave metrics for 1950–2005 are compared to observations at this local scale and then extended over 2006–2100 for the two RCP scenarios (Fig. 4). We do not average the heat wave metrics across multiple grid points near city locations, as this can have the effect of averaging out local heat wave events, particularly those that form north and south of the Great Dividing Range in southeast Australia. While the CMIP5 models show promise in simulating the broad variations in the heat waves metrics across Australia, it should be noted that these finer-scale time series are shown for illustrative purposes. More robust future finer-scale projections for each city would need to be carried out using a suitable regional-scale model and proven downscaling techniques, which are beyond the scope of this study.

The models simulate little historical change in HWF across each city, consistent with the gridded observations, despite observed increases throughout the inland regions of southeast, central, and northeast Australia (Perkins and Alexander 2013). However, in a future warming world, substantial increases in HWF are seen over 2006–2100 across all three cities (Figs. 4a,d,g). The RCP4.5 projection for Sydney HWF by 2100 (~14 days per summer; Fig. 4a) is similar to that for Perth (Fig. 4g) and more than double the frequency for Melbourne (~6 days per summer; Fig. 4d). For RCP8.5, by 2100 HWF increases to more than 42 days per summer for Sydney, and 40 days per summer for Perth, while for Melbourne it reaches only 12 days per summer. Under the high emissions scenario, the MMM thus suggests that by 2100 Sydney and Perth will experience a 20-fold increase in the number of heat wave days compared to the present day, while Melbourne will experience a comparatively low sixfold increase. It should be noted, however, that the models show a tendency to overestimate HWF along Australia's eastern coast, including Sydney, compared to the observations (Figs. 1a,d). To what extent future heat waves across the eastern coast show a greater persistence in terms of their dynamical setup is important to confirm for these projections, but this is beyond the scope of this study.

It is interesting to note that for Sydney and Perth, the difference between the mitigation (RCP4.5) and non-mitigation (RCP8.5) scenarios is quite significant (14 versus >40 days per summer), although for Melbourne the difference is particularly small (i.e., there is a degree of overlap between RCP4.5 and 8.5), possibly reflecting similarities between the two scenarios in the nature of changes to synoptic events that lead to heat waves across the southeast.

Sydney and Perth also show the greatest change in HWD by 2100 (Figs. 4b,h), with the longest heat waves being 12–14 (~7) days in duration for RCP8.5 (4.5). The models project a shorter HWD of <6 days for both RCP4.5 and 8.5 scenarios by 2100 for Melbourne. For Sydney and Perth, the evolution of HWD follows a similar path for both RCPs until ~2050, after which there is a strong divergence (Figs. 4b,h). It is interesting to note that the HWD time series for Melbourne does

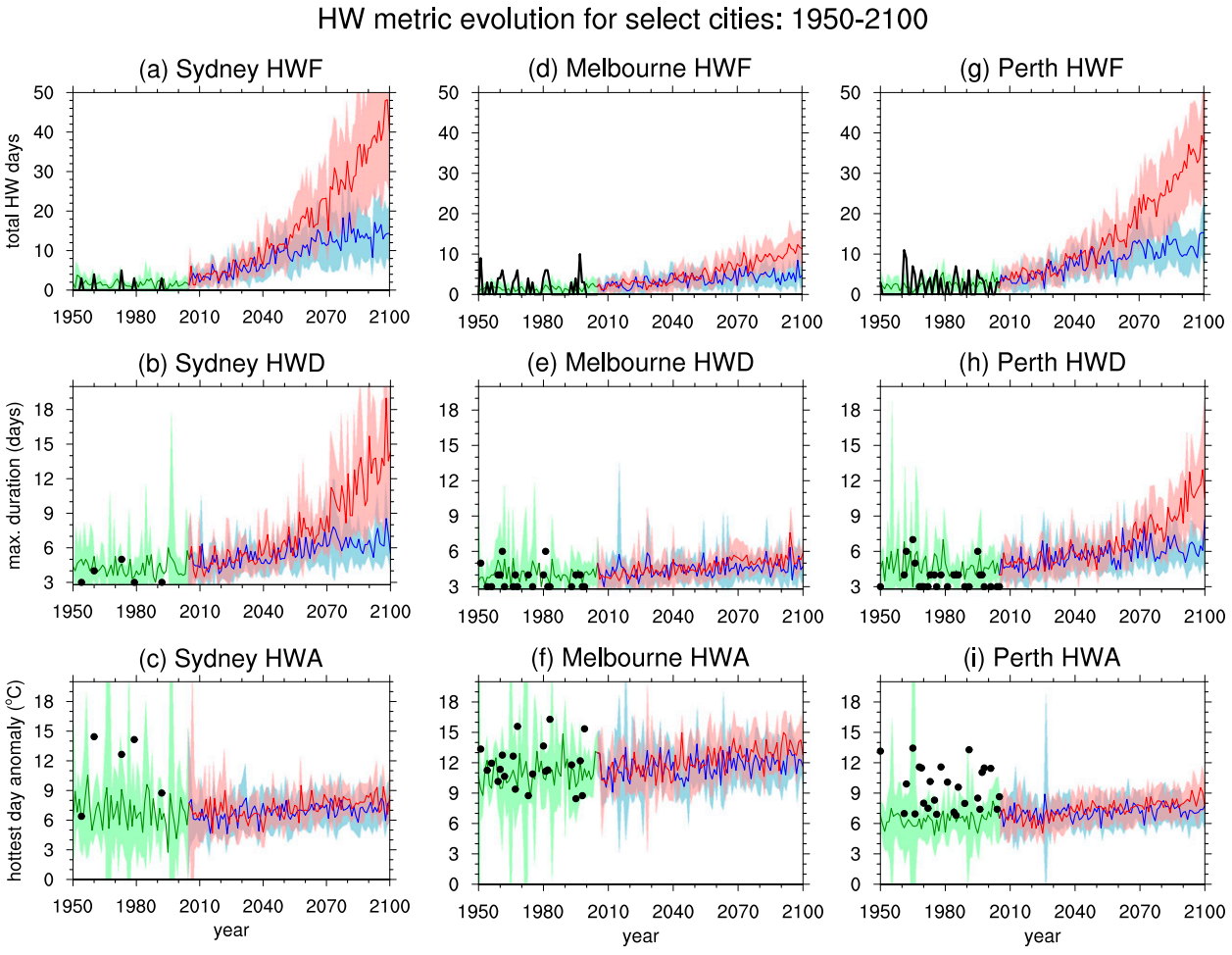

FIG. 4. Summer heat wave time series of (top) HWF, (middle) HWD, and (bottom) HWA. Observations (black) and CMIP5 historical (green) simulations are over 1950–2005, and CMIP5 RCP4.5 (blue) and RCP8.5 (red) simulations are over 2006–2100: (left) Sydney, (center) Melbourne, and (right) Perth. Shaded intervals indicate the 95% confidence interval. The observed HWD and HWA time series are discontinuous, so are shown with markers.

not diverge (Fig. 4e). This suggests there may be a physical limitation to the duration of heat waves in the southeast, possibly associated with the transient nature of blocking highs, and that this lack of increase in HWD contributes to the smaller increase in HWF seen for this region.

The future changes in HWA appear somewhat less dramatic across the three cities than for HWF and HWD (Figs. 4c,f,i). This is particularly so for Sydney and Perth, where the models also tend to underestimate the observed historical HWA (Figs. 4c,i). For Melbourne, the models show a slight improvement, but still slightly underestimate HWA during the twentieth century (Fig. 4f). The evolution of warming in all three cities for both RCP scenarios is similar; for Sydney there is minimal warming in RCP4.5 by 2100 and ~1°–2°C increase in HWA under RCP8.5, but there is quite substantial overlap with RCP4.5. For Melbourne and Perth the separation between the HWA time series for RCP4.5 and 8.5 is more obvious, particularly near 2100. The RCP8.5 HWA projection for Melbourne by 2100 is 14°C, almost 3°C above the 2005 simulated anomaly, while Perth is projected to experience a smaller HWA change of ~1.5°C for RCP8.5 (corresponding to a HWA of 8°–9°C by 2100). Of note is the decline in HWA variability in the twenty-first century, particularly for Sydney. This is most likely due to the increased frequency of simulated heat waves compared to the historical period. When no heat wave is recorded for a given year the HWA is not defined; as more heat waves are simulated in the future projections, particularly borderline events that just surpass the historical threshold, this acts to reduce HWA variability.

g. Future changes in winter warm spells

Observed trends in the seasonality of heat waves (and warm spells) across Australia (and globally) suggest that

changes in heat waves outside of the summer months occur over a broader spatial area and exhibit a greater magnitude of change relative to summer heat waves (Perkins et al. 2012). To gain insight into the seasonality of projected changes, we therefore analyze the changes in winter warm spell metrics across Australia over the end of the twenty-first century in the two RCP scenarios.

Figures 5a and 5d highlight the change in winter HWF for RCP4.5 and 8.5, respectively. The most noticeable difference to summer heat waves is the substantial increase in winter HWF along the southern and eastern coastal fringes, with parts of New South Wales, Victoria, and southwest Western Australia experiencing an increase of 15–25 days per winter (more than 10 times the historical HWF) for RCP4.5. This winter HWF increase is amplified to ≥40 days per winter for RCP8.5. Tasmania also sees a large increase in winter HWF of ≥50 (30–35) days per winter for RCP8.5 (4.5). Across northern and central Australia the meridional gradient of change is amplified in winter compared to summer, with the northern tropics projected to experience 50 (>30) days per winter for RCP8.5 (4.5). The winter HWF pattern of change is also less zonal for winter compared to summer for RCP8.5, with strong coastal gradients present along the southeast and southwest regions.

The spatial increases in winter HWD are quite similar to those of winter HWF (Figs. 5b,e). Warm spells south of 25°S (with the exception of Tasmania) are projected to increase by 2–4 days for RCP4.5. The gradient substantially increases north of 20°S, with the northern tropics projected to see increases in winter HWD of ≥14 days by 2100 compared to the historical period. For RCP8.5, these changes are amplified, particularly along coastal regions (all exhibiting strong onshore gradients). For southeast and southwest Australia, winter HWD increases by 12–14 days. From 20° to 30°S, a strong meridional gradient of change is evident, with winter HWD increases ranging from 6 days (at 30°S in central Australia) to >20 days (at 20°S). North of 20°S, the change in winter HWD reaches >40 days, consistent with previous studies suggesting that tropical regions will face an unprecedented heat regime in the coming decades, compared to higher-latitude regions (e.g., Diffenbaugh and Scherer 2011). The results are also consistent with a significant projected increase in the total number of tropical nights >20°C for northern Australia, which are more pronounced for RCP8.5 than for RCP4.5 (Sillmann et al. 2013).

As with summer HWA, winter HWA also shows the largest increase over southern Australia; however, as for the winter historical climatology, the maximum center of heat is located farther north than for summer (Figs. 5c,f). Across the southern Australian interior the winter HWA increases by 1.6°–2°C for RCP4.5 and up to 4°C for RCP8.5. Southeast, southwest, and northeast Australia show minimum increases in winter HWA, which most likely represents transient synoptic activity (southern regions) and air–sea interactions (northern regions).

In summary, for winter warm spells, the models project significant increases in frequency and duration across all of Australia, particularly for coastal regions, and more so than for summer. Furthermore, warm spells will be hotter in the future, with events exhibiting a greater rise in temperature than for summer heat waves, particularly across the southern interior. These projections for winter are also consistent with observed trends (Perkins et al. 2012).

h. Winter time series of heat wave metrics

The results in the previous section are complemented by examining the evolution of winter warm spell metrics for Sydney, Melbourne, and Perth. As expected, the largest changes in the cities' HWF also occurs during winter (Figs. 6a,d,g). Sydney is projected to experience a winter HWF >50 days per winter (~30 days per winter) by 2100 under the RCP8.5 (4.5) scenario, compared to 2 days per winter in the historical period (Fig. 6a). Perth will also experience a large winter HWF by 2100, increasing to 50 days per winter (20 days per winter) in RCP8.5 (4.5), compared to <2 days in the historical period (Fig. 6g). Although the summer HWF increase for Melbourne is much less than for Perth and Sydney, the increase in a winter HWF is considerable (Fig. 6d); RCP8.5 projections suggest that the winter HWF for Melbourne will reach ~40 days per winter by 2100, compared to ~2 days per winter in the historical period. However, through mitigation (RCP4.5) Melbourne might only experience 8 days per winter by 2100, highlighting the large asymmetry in the impact of warming on the frequency of winter events.

For the RCP8.5 scenario, Perth and Melbourne's winter HWF diverges from the RCP4.5 time series at ~2050, and Sydney's diverges at ~2060 (although with a small overlap between the two scenarios' uncertainty measures). This suggests that much of the impact of future climate change on warm spells occurs in the latter part of the twenty-first century, reflecting the large inertia in the climate system in response to greenhouse warming. The analysis also suggests the difference between RCP4.5 and 8.5 on winter HWF is smaller for Sydney (25 days per winter) than for Perth and Melbourne (30 days per winter), highlighting the complexity in making accurate future projections for potentially affected communities.

The results for HWD follow a similar evolution to HWF, with Sydney to potentially experience warm spells of length >30 days (10 days) by 2100 for RCP8.5 (4.5),

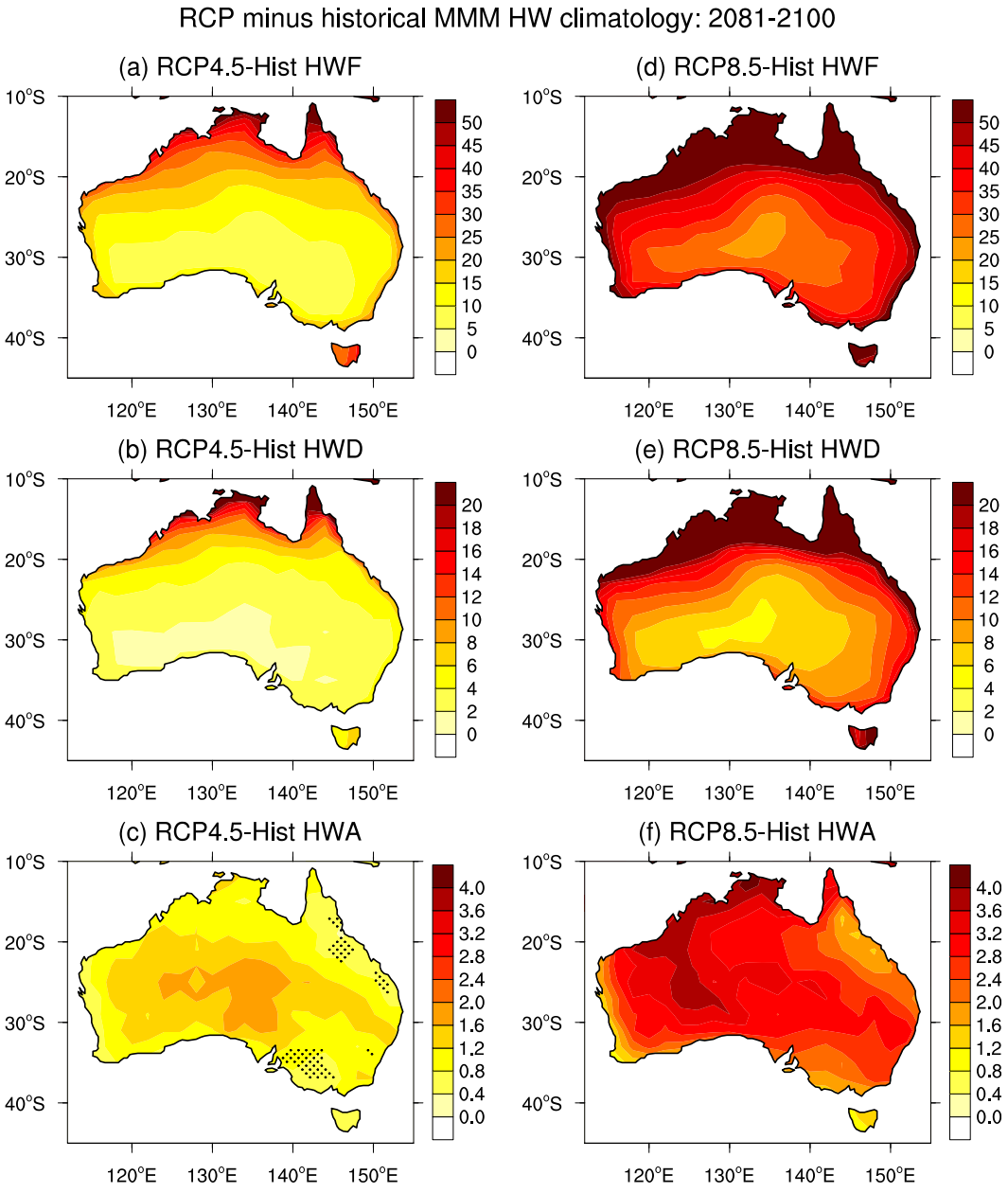

FIG. 5. As in Fig. 3, but for winter warm spells.

compared to 4 days in the historical period (Fig. 6b). Both Melbourne and Perth potentially experience smaller winter HWD increases compared to Sydney by 2100 (Figs. 6e,h). Melbourne's longest warm spells increase from 4 days in the historical period to 15 days (5 days) by the end of the century for RCP8.5 (4.5), while Perth experiences longer warm spells of 20 days (8 days) by 2100 for RCP8.5 (4.5). These results highlight the effectiveness of mitigation for the more southerly positioned cities such as Melbourne and Adelaide (not shown), and even suggest that winter HWD may have an effective ceiling of 10 days for Sydney, which occurs around 2050 for RCP4.5 and does not increase out to 2100. However, in the most extreme scenario, RCP8.5, the models project continued growth in the longest warm spells, although there is an indication of a plateau at the end of the century for Melbourne.

In Sydney, there is a noticeable divergence of HWA between RCP4.5 and 8.5 by ~2080, with the hottest winter events projected to reach an anomaly of 7°C for RCP8.5 (Fig. 6c), a statistically significant change from the end of the twentieth century for this region (Fig. 5f). Melbourne

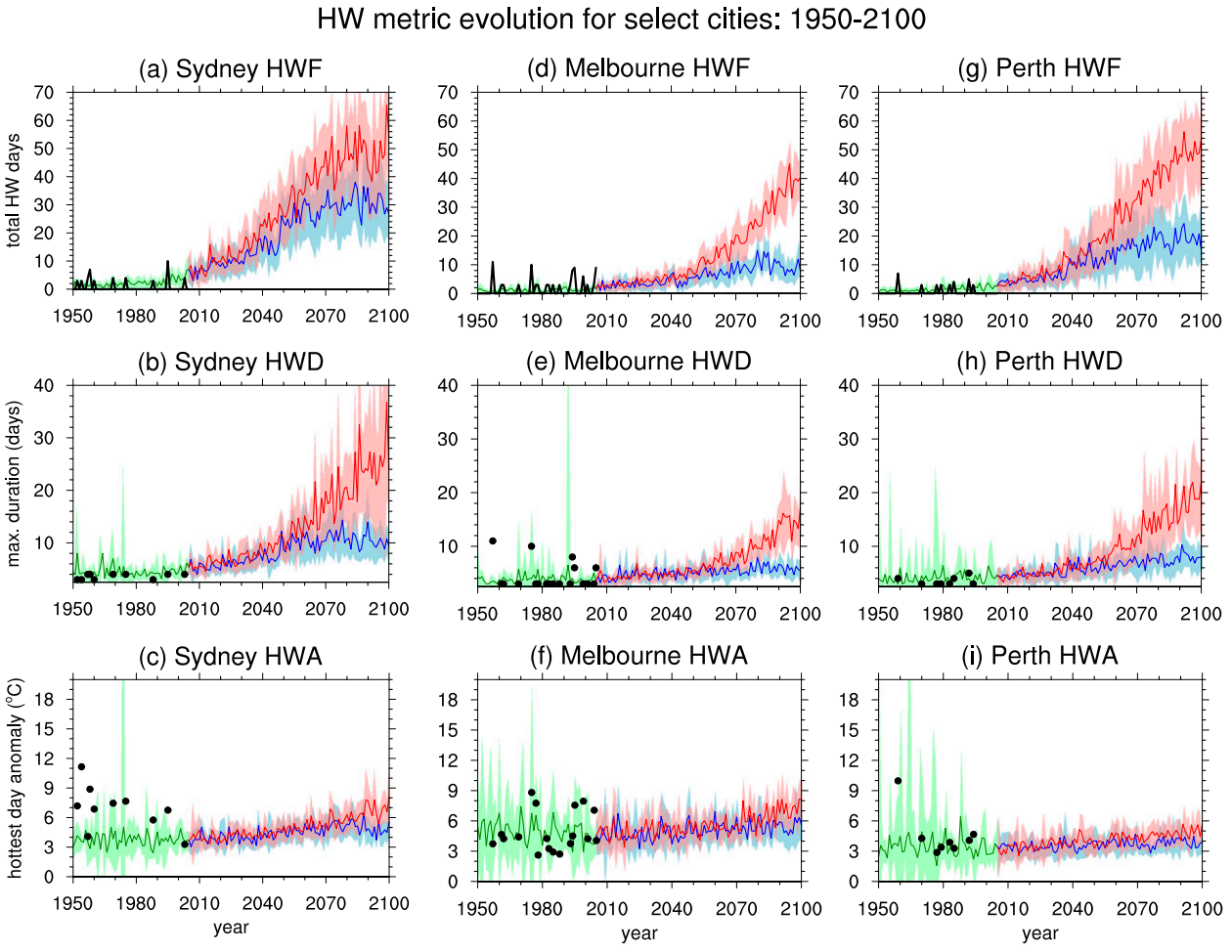

FIG. 6. As in Fig. 4, but for winter warm spells.

experiences a less noticeable divergence in HWA between the two RCP scenarios: HWA time series diverge by 2090, increasing to 8°C (6°C) for RCP8.5 (RCP4.5) by 2100 (Fig. 6f). Perth shows the smallest future changes in HWA (Fig. 6i), despite the trends in both RCP scenarios being statistically significant. As with summer HWA, we see a large reduction in variability for all three cities, although this is quite apparent for Perth. This is possibly due to more models projecting an increased number of future warm spells (i.e., virtually no future winters without a recorded HWA). In effect, this reduces the variance of HWA relative to the historical period. Nevertheless, the results for these city locations imply that winter warm spells will warm faster than summer heat waves under RCP8.5 for Sydney and Melbourne, whereas there are less obvious trends for RCP4.5 in all three cities.

i. Seasonality of future changes

From the above assessment, it is evident that projected changes in the various heat wave and warm spell metrics vary both spatially and seasonally. To gain further insight into the seasonality of projected changes, Fig. 7 displays the MMM spatial distribution of the season of maximum change in HWF, HWD, and HWA. For each grid point, the change in heat wave metrics over 2081–2100 relative to 1950–2005 in each season (summer, autumn, winter, and spring) is determined, and the season showing the greatest increase is displayed.

Changes in HWF and HWD show similar patterns: for RCP4.5 (Figs. 7a,b) winter is the season that exhibits the greatest change across southern Australia and along coastal regions for most of the continent (except northeast Queensland). For the southern central interior and northern central region the seasons of greatest change are split between summer and spring, respectively (although these patterns are reversed in Queensland). Isolated grid points in central and northern Australia show maximum changes in HWD during autumn. For RCP8.5 the largest changes in HWF and

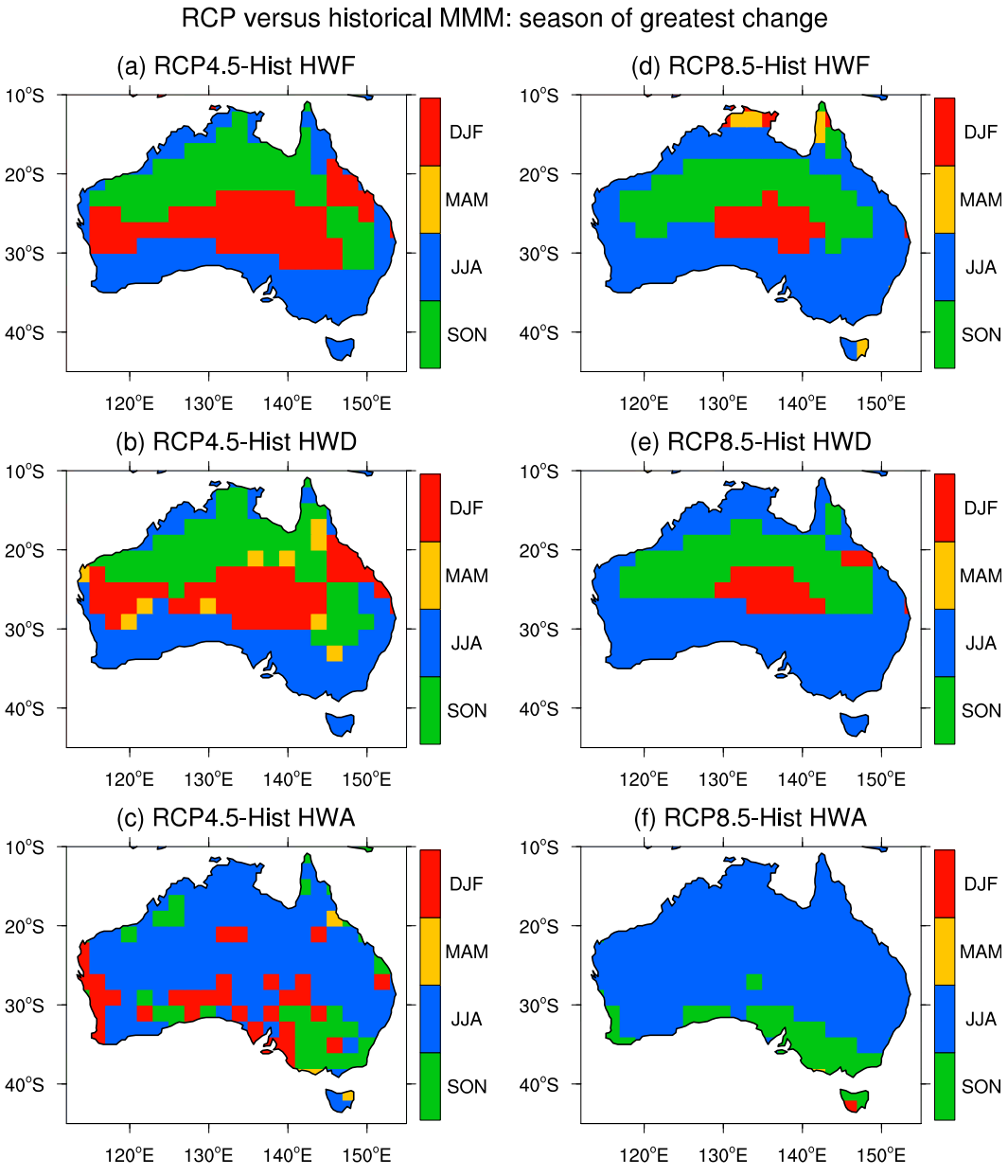

FIG. 7. Seasons of the greatest heat wave metric change for 2081–2100 compared to 1950–2005, for (left) RCP4.5 and (right) RCP8.5: (a),(d) HWF, (b),(e) HWD, and (c),(f) HWA. Red indicates summer (December–February), yellow autumn (March–May), blue winter (June–August), and green spring (September–November).

HWD (Figs. 7d,e) closely match RCP4.5, although the regions where winter changes are the greatest cover a wider area, replacing the regions of maximum summer and spring changes. In particular, the region where summer changes are a maximum is isolated to a small part of central Australia under this scenario.

As with the climatology, HWA displays a different pattern to HWF and HWD. For both RCP4.5 and 8.5 (Figs. 7c,f), the maximum increase in HWA across the majority of the continent occurs in winter. This is consistent with globally averaged observations, which show that when considering a daily T_{max} threshold definition, winter warm spells are warming faster than summer heat waves (Perkins et al. 2012). Across many midlatitude regions such as southern Australia and Europe, the frequency of warm days (T_{max} above the daily 90th percentile) is warming more strongly in winter than during summer (Donat et al. 2013). The strong increase in winter HWA is also consistent with model simulations that show the Indian Ocean dipole trending

toward a more positive phase, during which convection shifts away from eastern equatorial Indian Ocean (Cai et al. 2013). The positive dipole phase is associated with reduced cloudiness and drier conditions for much of southern Australia in winter, resulting in warmer daytime temperatures (Cai et al. 2011b). Across southern Australia, the maximum increase in HWA is seen during spring and summer for RCP4.5, but is limited to spring in RCP8.5. In general, the season of maximum change in HWA seems to represent an amplification of the climatological variations in HWA across the continent: HWA is maximum across southern latitudes in the warm seasons and farther north in the cool season (Figs. 1f, 2f).

j. Nonstationary threshold temperatures

We next investigate how nonstationary threshold temperatures affect the evolution of heat waves across Australia. We use a centered 31-yr sliding window (sufficient to filter out interannual variability) to calculate the threshold temperatures, rather than the fixed 1950–2005 climatology. For example, the threshold temperatures for 1980 are based on 1965–95 climatology. Based on data availability, the threshold temperatures for the first and last 16 years are based on fixed windows (1950–80 and 2070–2100, respectively). We also use a centered 31-yr sliding window to calculate the monthly-mean T_{max}, against which the anomalies for HWA are determined.

Results presented are differences with respect to the historical period 1965–90 (rather than 1950–2005 as in Figs. 3 and 5), as a true sliding climatology can be calculated for this period, and sliding thresholds are not contaminated with RCP data. Nevertheless, using 1950–2005 generates near-identical results, as there are minimal temperature trends over this period (not shown). Likewise, results from the future period 2066–85 are presented (rather than 2081–2100 as in Figs. 3 and 5), as again a true sliding climatology can be calculated for this period. Results for 2081–2100 are not shown because in the late twenty-first century, particularly under the RCP8.5 scenario, there are large temperature trends, and temperatures near 2100 are substantially above the 31-yr climatology centered on 2085, leading to spurious results.

Assessing heat waves relative to a nonstationary climatology effectively removes increases in the simulated HWF and HWD for both summer and winter, under both emission scenarios (Figs. 8a,b,d,e and 9a,b,d,e). This implies that the mean state change in these metrics is the dominant signal. However, for HWA we see a weak increase across southern Australia for summer under both RCP scenarios (Figs. 8c,f) and a stronger increase in winter (Figs. 9c,f). This implies that across southern Australia, the hottest daily T_{max} of the hottest heat waves (i.e., HWA) is increasing at a faster rate than the mean T_{max} is increasing, although such HWA increases are only significant at the 95% confidence level for a few isolated regions. Synoptic conditions conducive to heat waves in coastal areas tend to involve hot air from central Australia being directed toward the region of interest. Since mean temperatures in central Australia are projected to increase faster than coastal regions (not shown), this may explain how HWA can increase faster than the mean temperature across southern Australia, where desert lies to the north.

The strength of the HWA increase for southern Australia in RCP8.5 during summer is marginally stronger than RCP4.5, and includes a greater area of significance. Results suggest that by 2066–85 heat waves will have increased ~0.5°–1°C above the mean T_{max} increases, which are ~4°–5°C for RCP8.5 (not shown), with the largest increase along central-southern regions (Fig. 8f). This HWA increase is more extensive for winter warm spells (Fig. 9f), spreading farther east and west along southern coastal Australia, with increases >1°C above the mean T_{max} increase (~5°–6°C for RCP8.5; not shown). Despite the lack of significance, these findings suggest that in some regions the extreme maximum temperatures will increase at a faster rate than the overall mean state, even in the absence of an apparent increase in the total number of heat waves relative to that period's specific climatology. This is more pronounced for winter warm spells in southern Australia, although it should be noted that, aside from the city of Adelaide, many of these regions are sparsely populated.

4. Discussion and conclusions

CMIP5 projections for Australia indicate that more frequent, hotter, and longer summer heat waves and winter warm spells will occur by the end of the twenty-first century, with more extreme conditions under RCP8.5 compared to RCP4.5. The largest heat wave frequency and duration changes are projected to occur across the northern tropical regions of Australia, consistent with other studies into heat extremes across the globe (Diffenbaugh and Scherer 2011; Sillmann et al. 2013), while the maximum temperature of southern Australian heat waves increases more than for those in the north. In general, the CMIP5 models adequately simulate the observed heat wave climatologies over the late twentieth and early twenty-first centuries, although they tend to simulate an overly zonal climatological spatial pattern for frequency and duration, which places a degree of uncertainty on their projected changes in the

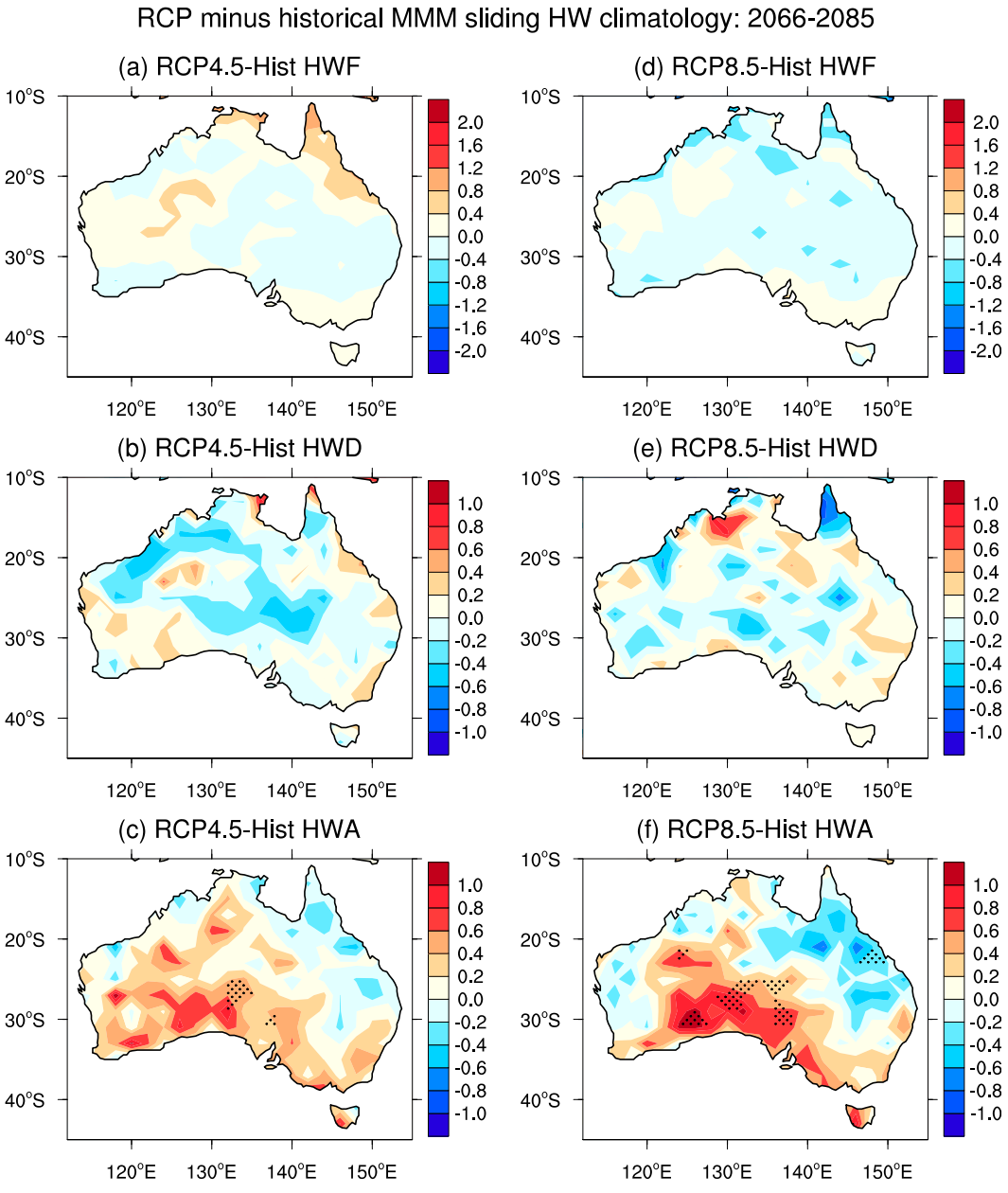

FIG. 8. Summer heat wave metric increases over 2066–85, compared to the 1965–90 climatology, based on nonstationary threshold climatologies, for (left) RCP4.5 and (right) RCP8.5: (a),(d) HWF, (b),(e) HWD, and (c),(f) HWA. A centered 31-yr sliding window is utilized to calculate the threshold temperatures rather than the fixed historical climatology (see main text for details). Stippling indicates where the 2066–85 and 1965–90 climatologies *are* significantly different at the 95% confidence level based on a Mann–Whitney *U* test.

twenty-first century (Figs. 1 and 3). The MMM performs better at simulating the observed amplitude of heat waves, and thus there is greater confidence in the simulated increases in the future. Consistent with observations of heat waves along southern Australia, the models simulate little frequency increase for southern Australian cities over 1950–2005 (Fig. 4); however, they simulate a 6- to 20-fold frequency increase in summer and a noticeable increase in summer duration by 2100 for RCP8.5.

The seasonality of projected heat wave changes suggests that a larger increase in the frequency and duration of heat waves will occur during austral winter across the populated regions of Australia, including the southern

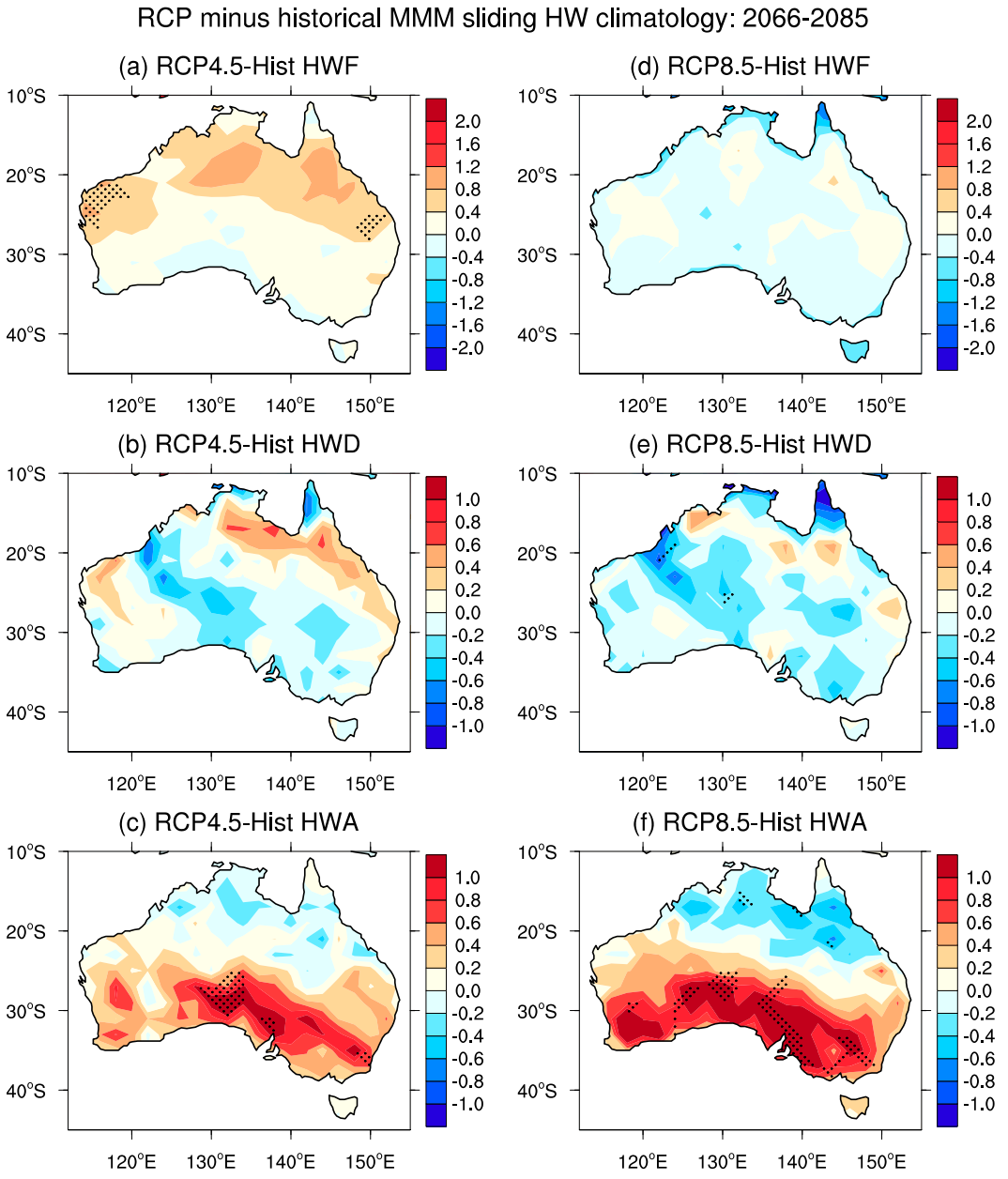

FIG. 9. As in Fig. 8, but for winter warm spells.

Murray–Darling basin, compared to any other season (Fig. 7). For the central and northern interior the models project the largest changes in spring and summer heat waves. Conversely, changes in hottest seasonal heat waves are largest in winter, except across southern regions, where the largest changes are seen during spring (southeast Australia) and summer (southwest and southern Australia in RCP4.5). This seasonality largely mirrors the spatial variations in the climatology, which exhibit a higher frequency and longer duration of summer heat waves across northern Australia, but higher amplitude summer heat waves across southern Australia (Fig. 1). As such, results suggest that, along with the substantial increase in the frequency, duration, and maximum temperature of heat waves during the twenty-first century, the seasonality and spatial variation of heat waves will become enhanced. For populated regions such as southeast and southwest Australia, the greatest increase in the hottest heat waves occurs in spring, consistent with a trend toward more positive Indian Ocean dipole events that often lead to severe summer bushfires (Cai et al. 2009).

The main cause of these future heat wave trends is the continued robust warming of the globe as a result of anthropogenic greenhouse gas emissions (e.g., Lewis and Karoly 2013). The amplification of atmospheric circulation patterns may also force additional changes in the intensity and frequency of heat waves, as simulated for regions in Europe and North America (Meehl and Tebaldi 2004). Studies using CMIP3 models suggest that due to global warming the local subtropical ridge intensity over Australia will increase over the twenty-first century (Timbal and Drosdowsky 2013), while the ridge position will shift poleward (Kent et al. 2013), reducing rainfall in southeastern Australia. Drier winters are also projected across southwest Australia in the twenty-first century (Cai et al. 2011a), with below average rainfall often associated with higher maximum temperatures (Nicholls 2004). This may account for the largest simulated increase in warm spells occurring during austral winter, as well as the fact that maximum temperatures in winter have a smaller range than for summer (i.e., a narrower probability distribution function; not shown). Despite model biases, atmospheric blocking is expected to increase in the summer months in the Tasman Sea (Grose et al. 2012) east of southeast Australia, which is consistent with more summer heat waves in the future for southeast Australia (Sadler et al. 2012). However, a future Tasman Sea warming and positive southern annular mode trend are also likely to promote increased summer rainfall over southeast Australia (Shi et al. 2008), which may account for the weaker increase in summer HWF in Melbourne compared to Perth and Sydney (Fig. 4). For the northern tropics, while the summer monsoon domain is not expected to change significantly in the future, despite a general projected increase in summer rainfall (Wang et al. 2013), the monsoon is expected to experience onset delays and shortened durations (Zhang et al. 2012), which may partially explain the large frequency and duration increases in this region.

A robust result from this study is that summer heat waves and winter warm spells will increase in frequency, duration, and amplitude across Australia, and this increase is strongly proportional both to the emission scenario, and to the latitude of a particular region (i.e., tropical versus extratropical). In addition, even if the heat waves are referenced to a warming mean state, the hottest events will gradually become hotter by the end of this century over southern Australia, particularly during winter and for the RCP8.5 high emission scenario. While there are obvious human benefits for an increase in winter warm spells, such as reduced disease and fatalities (McMichael et al. 2006), adverse effects to temperature-dependent agriculture are also likely (e.g., Turner et al. 2011). Furthermore, increases in summer heat waves and temperatures will have severe adverse effects to human health (e.g., Kyselý 2010; Sherwood and Huber 2010), as well as ecosystems and agriculture (Coumou and Robinson 2013, and references therein). While the temporal evolution of heat waves has been established, it is still not well understood whether a change in heat waves across southern Australia is manifested through a change in the mean-state temperature alone, or in part due to atmospheric and oceanic circulation changes. A companion study will investigate circulation and sea surface temperature patterns prior to and during summer heat waves, to gain better insight into how dynamics during summer heat waves across southern Australia will change in a warming world.

Acknowledgments. This research is supported by the Goyder Institute for Water Research, and the Australian Climate Change Science Program. A. Pezza acknowledges the financial support of the Australian Research Council through Discovery Project DP120103950. S. Perkins is supported through the Australian Research Council Centre of Excellence for Climate System Science, CE110001028. We thank Peter van Rensch and two anonymous reviewers for their valuable comments that improved the manuscript. We acknowledge the World Climate Research Programme's Working Group on Coupled Modelling, which is responsible for CMIP, and thank the climate modelling groups (listed in Table 1 of this paper) for producing and making their model output available.

REFERENCES

Alexander, L. V., and Coauthors, 2013: Summary for policymakers. *Climate Change 2013: The Physical Science Basis,* T. F. Stocker et al., Eds., Cambridge University Press, 3–29. [Available online at http://www.climatechange2013.org/images/report/WG1AR5_SPM_FINAL.pdf.]

Barriopedro, D., E. M. Fischer, J. Luterbacher, R. M. Trigo, and R. Garcia-Herrera, 2011: The hot summer of 2010: Redrawing the temperature record map of Europe. *Science,* **332,** 220–224, doi:10.1126/science.1201224.

Berckmans, J., T. Woollings, M.-E. Demory, P.-L. Vidale, and M. Roberts, 2013: Atmospheric blocking in a high resolution climate model: Influences of mean state, orography and eddy forcing. *Atmos. Sci. Lett.,* **14,** 34–40, doi:10.1002/asl2.412.

Bumbaco, K. A., K. D. Dello, and N. A. Bond, 2013: History of Pacific Northwest heat waves: Synoptic pattern and trends. *J. Appl. Meteor. Climatol.,* **52,** 1618–1631, doi:10.1175/JAMC-D-12-094.1.

Bureau of Meteorology, 2013: A prolonged autumn heatwave for southeast Australia. Bureau of Meteorology Special Climate Statement 45, 11 pp. [Available online at http://www.bom.gov.au/climate/current/statements/scs45.pdf.]

Cai, W., T. Cowan, and M. Raupach, 2009: Positive Indian Ocean dipole events precondition southeast Australia bushfires. *Geophys. Res. Lett.,* **36,** L19710, doi:10.1029/2009GL039902.

——, P. van Rensch, S. Borlace, and T. Cowan, 2011a: Does the Southern Annular Mode contribute to the persistence of the multidecade-long drought over southwest Western Australia? *Geophys. Res. Lett.,* **38,** L14712, doi:10.1029/2011GL047943.

——, ——, T. Cowan, and H. Hendon, 2011b: Teleconnection pathways of ENSO and the IOD and the mechanisms for impacts on Australian rainfall. *J. Climate,* **24,** 3910–3923, doi:10.1175/2011JCLI4129.1.

——, X.-T. Zheng, E. Weller, M. Collins, T. Cowan, M. Lengaigne, W. Yu, and T. Yamagata, 2013: Projected response of the Indian Ocean dipole to greenhouse warming. *Nat. Geosci.,* **6,** 999–1007, doi:10.1038/ngeo2009.

Carril, A., S. Gualdi, A. Cherchi, and N. Navarra, 2008: Heatwaves in Europe: Areas of homogeneous variability and links with the regional to large-scale atmospheric and SSTs anomalies. *Climate Dyn.,* **30,** 77–98, doi:10.1007/s00382-007-0274-5.

Coumou, D., and S. Rahmstorf, 2012: A decade of weather extremes. *Nat. Climate Change,* **2,** 491–496, doi:10.1038/nclimate1452.

——, and A. Robinson, 2013: Historic and future increase in the global land area affected by monthly heat extremes. *Environ. Res. Lett.,* **8,** 034018, doi:10.1088/1748-9326/8/3/034018.

Della-Marta, P., J. Luterbacher, H. von Weissenfluh, E. Xoplaki, M. Brunet, and H. Wanner, 2007: Summer heat waves over western Europe 1880–2003: Their relationship to large-scale forcings and predictability. *Climate Dyn.,* **29,** 251–275, doi:10.1007/s00382-007-0233-1.

Diffenbaugh, N. S., and M. Scherer, 2011: Observational and model evidence of global emergence of permanent, unprecedented heat in the 20th and 21st centuries. *Climatic Change,* **107,** 615–624, doi:10.1007/s10584-011-0112-y.

Ding, Y. H., G. Y. Ren, Z. C. Zhao, Y. Xu, Y. Luo, Q. P. Li, and J. Zhang, 2007: Detection, causes and projection of climate change over China: An overview of recent progresses. *Adv. Atmos. Sci.,* **24,** 954–971, doi:10.1007/s00376-007-0954-4.

Donat, M. G., and Coauthors, 2013: Updated analyses of temperature and precipitation extreme indices since the beginning of the twentieth century: The HadEX2 dataset. *J. Geophys. Res. Atmos.,* **118,** 2098–2118, doi:10.1002/jgrd.50150.

Ellis, S., P. Kanowski, and R. Whelan, 2004: National inquiry on bushfire mitigation and management. Council of Australian Governments Tech. Rep., 451 pp. [Available online at http://www.dfes.wa.gov.au/publications/GeneralReports/FESA_Report-NationalInquiryonBushfireMitigationandManagement.pdf.]

Fischer, E. M., and C. Schar, 2010: Consistent geographical patterns of changes in high-impact European heatwaves. *Nat. Geosci.,* **3,** 398–403, doi:10.1038/ngeo866.

Gosling, S., G. McGregor, and J. A. Lowe, 2009: Climate change and heat-related mortality in six cities. Part II: Climate model evaluation and projected impacts from changes in the mean and variability of temperature with climate change. *Int. J. Biometeor.,* **53,** 31–51, doi:10.1007/s00484-008-0189-9.

Grose, M. R., I. Barnes-Keoghan, S. P. Corney, C. J. White, G. K. Holz, J. B. Bennett, S. M. Gaynor, and N. L. Bindoff, 2010: Climate futures for Tasmania: General climate impact. Antarctic Climate and Ecosystems Cooperative Research Centre Tech. Rep., 68 pp. [Available online at http://www.acecrc.org.au/Research/Climate+Futures.]

——, M. Pook, P. McIntosh, J. Risbey, and N. Bindoff, 2012: The simulation of cutoff lows in a regional climate model: Reliability and future trends. *Climate Dyn.,* **39,** 445–459, doi:10.1007/s00382-012-1368-2.

Hansen, J., M. Sato, and R. Ruedy, 2012: Perception of climate change. *Proc. Natl. Acad. Sci. USA,* **109,** E2415–E2423, doi:10.1073/pnas.1205276109.

Hao, Z., A. AghaKouchak, and T. J. Phillip, 2013: Changes in concurrent monthly precipitation and temperature extremes. *Environ. Res. Lett.,* **8,** 034014, doi:10.1088/1748-9326/8/3/034014.

Hudson, D., A. Marshall, and O. Alves, 2011: Intraseasonal forecasting of the 2009 summer and winter Australian heat waves using POAMA. *Wea. Forecasting,* **26,** 257–279, doi:10.1175/WAF-D-10-05041.1.

Jones, D., W. Wang, and R. Fawcett, 2009: High-quality spatial climate data-sets for Australia. *Aust. Meteor. Oceanogr. J.,* **58,** 233–248.

Karoly, D., 2009: The recent bushfires and extreme heat wave in south-east Australia. *Bull. Austr. Meteor. Oceanogr. Soc.,* **22,** 10–13.

Kent, D., D. Kirono, B. Timbal, and F. Chiew, 2013: Representation of the Australian sub-tropical ridge in the CMIP3 models. *Int. J. Climatol.,* **33,** 48–57, doi:10.1002/joc.3406.

Kyselý, J., 2010: Recent severe heat waves in central Europe: How to view them in a long-term prospect? *Int. J. Climatol.,* **30,** 89–109, doi:10.1002/joc.1874.

Lau, N.-C., and M. Nath, 2012: A model study of heat waves over North America: Meteorological aspects and projections for the twenty-first century. *J. Climate,* **25,** 4761–4784, doi:10.1175/JCLI-D-11-00575.1.

Le Tertre, A., and Coauthors, 2006: Impact of the 2003 heatwave on all-cause mortality in 9 French cities. *Epidemiology,* **17,** 75–79, doi:10.1097/01.ede.0000187650.36636.1f.

Lewis, S., and D. Karoly, 2013: Anthropogenic contributions to Australia's record summer temperatures of 2013. *Geophys. Res. Lett.,* **40,** 3705–3709, doi:10.1002/grl.50673.

Loughnan, M., N. Nicholls, and N. Tapper, 2010: Mortality–temperature thresholds for ten major population centres in rural Victoria, Australia. *Health Place,* **16,** 1287–1290, doi:10.1016/j.healthplace.2010.08.008.

Lyon, B., 2009: Southern Africa summer drought and heat waves: Observations and coupled model behavior. *J. Climate,* **22,** 6033–6046, doi:10.1175/2009JCLI3101.1.

Mann, H. B., and D. R. Whitney, 1947: On a test of whether one of two random variables is stochastically larger than the other. *Ann. Math. Stat.,* **18,** 50–60, doi:10.1214/aoms/1177730491.

Marshall, A. G., D. Hudson, M. C. Wheeler, O. Alves, H. H. Hendon, M. J. Pook, and J. S. Risbey, 2014: Intra-seasonal drivers of extreme heat over Australia in observations and POAMA-2. *Climate Dyn.,* doi:10.1007/s00382-013-2016-1, in press.

Mastrandrea, M., C. Tebaldi, C. Snyder, and S. Schneider, 2011: Current and future impacts of extreme events in California. *Climatic Change,* **109,** 43–70, doi:10.1007/s10584-011-0311-6.

McMichael, A., R. Woodruff, and S. Hales, 2006: Climate change and human health: Present and future risks. *Lancet,* **367,** 859–869, doi:10.1016/S0140-6736(06)68079-3.

Meehl, G., and C. Tebaldi, 2004: More intense, more frequent, and longer lasting heat waves in the 21st century. *Science,* **305,** 994–997, doi:10.1126/science.1098704.

Nairn, J. and R. Fawcett, 2013: Defining heatwaves: Heatwave defined as a heat-impact event servicing all community and

business sectors in Australia. CAWCR Tech. Rep. 60, 96 pp. [Available online at http://www.cawcr.gov.au/publications/technicalreports/CTR_060.pdf.]

Nguyen, H., A. Evans, C. Lucas, I. Smith, and B. Timbal, 2013: The Hadley circulation in reanalyses: Climatology, variability, and change. *J. Climate,* **26,** 3357–3376, doi:10.1175/JCLI-D-12-00224.1.

Nicholls, N., 2004: The changing nature of Australian droughts. *Climatic Change,* **63,** 323–336, doi:10.1023/B:CLIM.0000018515.46344.6d.

——, J. Uotila, and L. Alexander, 2010: Synoptic influences on seasonal, interannual and decadal temperature variations in Melbourne, Australia. *Int. J. Climatol.,* **30,** 1372–1381, doi:10.1002/joc.1965.

Parker, T. J., G. J. Berry, and M. J. Reeder, 2013: The influence of tropical cyclones on heat waves in southeastern Australia. *Geophys. Res. Lett.,* **40,** 6264–6270, doi:10.1002/2013GL058257.

Perkins, S. E., 2011: Biases and model agreement in projections of climate extremes over the tropical Pacific. *Earth Interact.,* **15**, doi:10.1175/2011EI395.1.

——, and L. V. Alexander, 2013: On the measurement of heat waves. *J. Climate,* **26,** 4500–4517, doi:10.1175/JCLI-D-12-00383.1.

——, and E. M. Fischer, 2013: The usefulness of different realizations for the model evaluation of regional trends in heat waves. *Geophys. Res. Lett.,* **40,** 5793–5797, doi:10.1002/2013GL057833.

——, L. V. Alexander, and J. R. Nairn, 2012: Increasing frequency, intensity and duration of observed global heatwaves and warm spells. *Geophys. Res. Lett.,* **39,** L20714, doi:10.1029/2012GL051120.

Pezza, A., P. van Rensch, and W. Cai, 2012: Severe heat waves in southern Australia: Synoptic climatology and large scale connections. *Climate Dyn.,* **38,** 209–224, doi:10.1007/s00382-011-1016-2.

Risbey, J., M. Pook, P. McIntosh, M. Wheeler, and H. Hendon, 2009: On the remote drivers of rainfall variability in Australia. *Mon. Wea. Rev.,* **137,** 3233–3253, doi:10.1175/2009MWR2861.1.

Sadler, K. J., A. Pezza, and W. Cai, 2012: Cool sea surface temperatures in the Tasman Sea associated with blocking and heatwaves in Melbourne. *Bull. Aust. Meteor. Oceanogr. Soc.,* **25,** 80–83.

Scaife, A. A., T. Woolings, J. Knight, G. Martin, and T. Hinton, 2010: Atmospheric blocking and mean biases in climate models. *J. Climate,* **23,** 6143–6152, doi:10.1175/2010JCLI3728.1.

Sherwood, S. C., and M. Huber, 2010: An adaptability limit to climate change due to heat stress. *Proc. Natl. Acad. Sci. USA,* **107,** 9552–9555, doi:10.1073/pnas.0913352107.

Shi, G., J. Ribbe, W. Cai, and T. Cowan, 2008: An interpretation of Australian rainfall projections. *Geophys. Res. Lett.,* **35,** L02702, doi:10.1029/2007GL032436.

Sillmann, J., V. V. Kharin, F. W. Zwiers, X. Zhang, and D. Bronaugh, 2013: Climate extremes indices in the CMIP5 multimodel ensemble: Part 2. Future climate projections. *J. Geophys. Res. Atmos.,* **118,** 2473–2493, doi:10.1002/jgrd.50188.

Taylor, K., R. Stouffer, and G. Meehl, 2012: An overview of CMIP5 and the experiment design. *Bull. Amer. Meteor. Soc.,* **93,** 485–498, doi:10.1175/BAMS-D-11-00094.1.

Timbal, B., and W. Drosdowsky, 2013: The relationship between the decline of southeastern Australian rainfall and the strengthening of the subtropical ridge. *Int. J. Climatol.,* **33,** 1021–1034, doi:10.1002/joc.3492.

Tong, S., C. Ren, and N. Becker, 2010: Excess deaths during the 2004 heatwave in Brisbane, Australia. *Int. J. Biometeor.,* **54,** 393–400, doi:10.1007/s00484-009-0290-8.

Trenberth, K., and J. Fasullo, 2012: Climate extremes and climate change: The Russian heat wave and other climate extremes of 2010. *J. Geophys. Res.,* **117,** D17103, doi:10.1029/2012JD018020.

Trigo, R., R. García-Herrera, J. Diaz, I. Trigo, and M. Valente, 2005: How exceptional was the early August 2003 heatwave in France? *Geophys. Res. Lett.,* **32,** L10701, doi:10.1029/2005GL022410.

Tryhorn, L., and J. Risbey, 2006: On the distribution of heatwaves over the Australian region. *Aust. Meteor. Mag.,* **55,** 169–182.

Turner, N., N. Molyneux, S. Yang, Y.-C. Xiong, and K. Siddique, 2011: Climate change in south-west Australia and north-west China: Challenges and opportunities for crop production. *Crop Pasture Sci.,* **62,** 445–456, doi:10.1071/CP10372.

Ummenhofer, C., and Coauthors, 2011: Indian and Pacific Ocean influences on southeast Australian drought and soil moisture. *J. Climate,* **24,** 1313–1336, doi:10.1175/2010JCLI3475.1.

Wang, B., S. Y. Yim, J. Y. Lee, J. Liu, and K. J. Ha, 2013: Future change of Asian–Australian monsoon under RCP 4.5 anthropogenic warming scenario. *Climate Dyn.,* **42,** 83–100, doi:10.1007/s00382-013-1769-x.

Wu, Z., Z. Jiang, J. Li, S. Zhong, and L. Wang, 2012a: Possible association of the western Tibetan Plateau snow cover with the decadal to interdecadal variations of northern China heatwave frequency. *Climate Dyn.,* **39,** 2393–2402, doi:10.1007/s00382-012-1439-4.

——, H. Lin, J. Li, Z. Jiang, and T. Ma, 2012b: Heat wave frequency variability over North America: Two distinct leading modes. *J. Geophys. Res.,* **117,** D02102, doi:10.1029/2011JD016908.

Zanobetti, A., and J. Schwartz, 2008: Temperature and mortality in nine US cities. *Epidemiology,* **19,** 563–570, doi:10.1097/EDE.0b013e31816d652d.

Zhang, H., P. Liang, A. Moise, and L. Hanson, 2012: Diagnosing potential changes in Asian summer monsoon onset and duration in IPCC AR4 model simulations using moisture and wind indices. *Climate Dyn.,* **39,** 2465–2486, doi:10.1007/s00382-012-1289-0.